Chaotic Modeling and Simulation (CMSIM) 4: 489-501, 2016

Second Observation of Quasi-Chaos in Erbium doped fiber ring laser

S. Zafar Ali

Department of Electrical Engineering, Air University, E-9 Islamabad, Pakistan
email ***zafarali@mail.au.edu.pk***

Abstract

This numerical investigation is motivated by the exciting recent discovery of quasi-chaos, in loss modulated erbium doped fiber ring laser (EDFRL), which looks like chaos but converges to single trajectory for widely separate initial conditions in physical phase space. Both pure and quasi-chaos are generated in pump modulated EDFRL using chaos message masking and additive chaos modulation configurations respectively, for comparison in different domains. Quasi-chaos has chaotic amplitude in time domain, rich spectral content in frequency domain, fractal physical phase space, and fast decreasing autocorrelation function. Sensitive dependence on initial conditions is numerically tested for both these chaos, with pure chaos diverging even for minute deviations while quasi-chaos converging even for extreme values of initial conditions. Lyapunov exponent of quasi-chaos, calculated with TISEAN, however, are still positive, as TISEAN works on time delay embedded phase space of single variable, which is shown fractal here. Quasi-chaotic pulses are periodic in time and chaotic in amplitude, with bunching of sub-pulses into super pulses with respective fixed periods. Quasi-chaos cannot be used for secure communication and experimental outputs in forced chaotic oscillators under noisy conditions need careful analysis. This evidence marks the confirmation of existence of fifth region of operation in nonlinear systems.

Keywords:

Quasi-chaos, Nonlinear dynamics of fiber laser, Pump modulation.

I Introduction

Chaos, quantum mechanics and theory of relativity are widely accepted as the three most important discoveries of 21st century. Chaos, which is mainly identified by its sensitive dependence on initial conditions, is a ubiquitous phenomenon in many nonlinear systems fulfilling Poincare Bendixon's criteria.

Received revised: 14 August 2016 / Accepted: 21 October 2016
 ISSN 2241-0503

The application of optical chaos in secure optical communication has reached successful results in Athens experiment [1] and yet new exciting aspects of optical chaos are being discovered [2, 3]. Optical chaos in EDFRL can be produced both in autonomous manner [4] and by periodic perturbations as in loss modulation [5-6] and pump modulation [7-14]. Recently quasi-chaos was discovered [3] in loss modulated EDFRL, which looked like chaos in time, frequency, phase space and autocorrelation signatures but violated the basic criteria of chaos i.e. sensitive dependence on initial conditions (SDIC) once the system, is numerically subjected to different initial conditions. Until first discovery [3] of quasi-chaos, nonlinear systems were earlier known to exhibit only four regions of operation i.e. chaos, periodic, stable and quasi-periodic with switching of regions being determined by the tuning of parameters and driving conditions.

There are three message encoding configurations possible in each of three mentioned schemes in EDFRL i.e. additive chaos modulation (ACM) where message gets entered into laser rate equations, chaos message masking (CMS) where message is not part of rate equations and is added in the last and chaos shift keying (CSK) where one parameter is switched with data. The message encoding scheme of loss modulated EDFRL reported earlier [5] as chaos message masking (CMS) was latter [6] corrected to be additive chaos modulation (ACM) scheme. The effect of message parameters (message frequency, amplitude and phase) on EDFRL chaos dynamics was studied in detail [6] and it was shown that one necessary condition of chaos generation is that message and modulating sine waves frequencies are not integral multiples of each other. However, the recent paper [3] has proven that the behaviour earlier identified as pure chaos in EDFRL ACM scheme [5,6], was in fact quasi-chaos, because it straightaway violates sensitive dependence on initial conditions. However, surprisingly it still looks like chaos in several domains and even renders positive lyapunov exponent using TISEAN [15]. The reason for this anomaly was identified [3] was the fractal nature of time-delayed embedded phase space of lasing field intensity. It was also shown [3] that in order to produce pure chaos, message had to be completely eliminated from EDFRL. Therefore, the factor responsible for generation of quasi chaos was the interplay of message and loss modulating frequencies within the laser cavity.

EDFRL pump modulation scheme shall be the next logical candidate for tracing the signs of quasi-chaos, because it is the next forced configuration of EDFRL which produces chaos. We will investigate both message encoding schemes i.e. chaos message masking and additive chaos modulation for generation of pure and quasi-chaos respectively, in the same stepwise manner as done earlier [3] in loss modulation scheme. We will specifically inspect the convergence of trajectories to same path in quasi-chaos for widely separated initial conditions. We shall also carry out all qualitative tests and quantitative test of Lyapunov exponent calculation on both chaos and evaluate the results. Once quasi-chaos is proven discovered second time here, it will be safe to assume that it is a ubiquitous phenomenon in all forced chaotic generators under similar conditions as identified earlier [3] and revalidated here. The paper is organised as follows. Section I provides introduction and literature review, followed by Section II mentioning the mathematical models and optical circuits of both configurations studied in this paper. Section III shows simulations and section IV discusses these results. Section V concludes the results and indicates their implications in research.

II Mathematical model

In this section are given the optical circuits and corresponding mathematical models of pump modulated EDFRL CMS and ACM schemes in Fig.1 (a)-(b) and Eq. 1(a)-(c) and Eq. 2 (a)-(d) respectively, the basic model adapted from Luo[14]. It is obvious from Fig.1 (a) and Eq.(1) that message is not part of loop dynamics and is added in the last to the chaos generated by loop in CMS. However, it can be seen in Fig. 1(a) and Eq.(2) that ACM has message sine wave being added into the loop thus modifying chaos dynamics.

$$\dot{E}_{LA} = -k_{a0}E_{LA} + g_a E_{LA} D_A + \xi_{LA} \tag{1a}$$

$$\dot{D}_A = -\frac{1}{\tau}[(1 + I_{PA} + E_{LA}^2)D_A - I_{PA} + 1] \tag{1b}$$

$$I_{PA} = I_{PA0}(1 + m_a \sin(\omega_a t_a)) \tag{1c}$$

$$\dot{E}_{LA} = -k_a(E_{LA} - c_a S_{in}) + g_a E_{LA} D_A + \xi_{LA} \tag{2a}$$

$$\dot{D}_A = -\frac{1}{\tau}[(1 + I_{PA} + E_{LA}^2)D_A - I_{PA} + 1] \tag{2b}$$

$$I_{PA} = I_{PA0}(1 + m_a \sin(\omega_a t_a)) \tag{2c}$$

$$S_{in} = S_0(1 - m_s \sin(\omega_s t)) \tag{2d}$$

where "." denotes time derivative, E_{LA} is the lasing field strength, D_A is population inversion density, τ is the Erbium meta-stable state decay time, ξ_{LA} is the spontaneous emission factor, I_{PA} is the pump power, k_{a0} is the cavity loss (decay rate), g_a is the cavity gain,, m_a is the modulation index, ω_a is the angular loss modulating frequency, S_0 is the message amplitude, c_a is the coupling strength of message and ω_s is the message frequency.

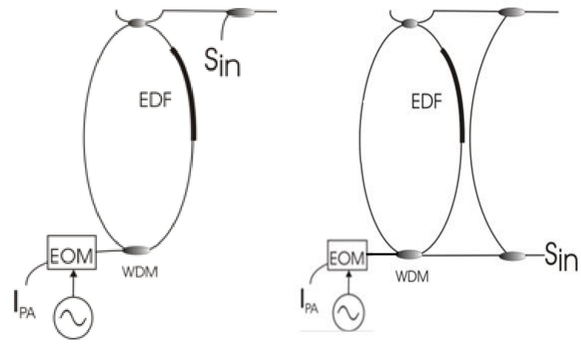

Fig.1 Pump modulation in EDFRL
(a) Chaos message Masking
(b) Additive Chaos Modulation

The values of model parameters used in simulations in following section are given in Table.1 below are same for CMS and ACM configurations except the last two are present in latter only. The numerical integration is performed using fourth order Runge-Kutta method with a step size of 10 nsec, in all simulations here, to ensure best accuracy of results. It may also be mentioned here that E_{LA0} and D_{A0} are the initial conditions for lasing field intensity and population inversion density here. The dynamic range is 0 to 150 a.u. for E_{LA0} and -1 to 1 for $D_{A0.}$

Table 1 Pump modulated EDFRL parameters for ACM and CMS

Parameter	**Symbol**	**Value**
Decay time metastable state	τ	10 ms
Spontaneous emission factor	ξ_{LA}	10^{-4}
Pump power	I_{PA0}	20 mW
Modulation index	m_a	0.94
Cavity loss / Decay rate	k_{a0}	$6.46\text{x}10^{6}$
Pump Modulation frequency	ω_a	2π x 9 x10^{3}
Message frequency	ω_s	2π x 3.1919 x10^{3}
Message Amplitude	S_0	1
Coupling ratio	c_a	0.02

III Simulations results

Initially the CMS model of Eq.1(a)-(c) is simulated using parameters as given in Table.1. The results are plotted in Fig. 2 for minutely varying initial conditions with Fig.2 (a) taken as reference i.e. E_{LA0}=0 and D_{A0}=0.47. E_{LA0} is kept at zero and D_{A0} is varied to 0.470001, 0.47001 and 0.4701 in Fig.2 (b)-(d) and the point of change in chaos signature with reference to Fig.2 (a) is marked by an arrow in last three diagrams. There are two important observations made here Firstly, the chaos outputs are different in all figures, even for the smallest change of 10^{-6} in D_{A0} in Fig.2 (b) which is quite in line with SDIC and is as expected for a pure chaos. Secondly, the starting time of change in chaos as marked by arrow shifts to right with the gradual increase in difference of D_{A0} from value of 0.47 which is again as expected. Both of these observations are well known for a pure chaos and are responsible for its long-term unpredictability.

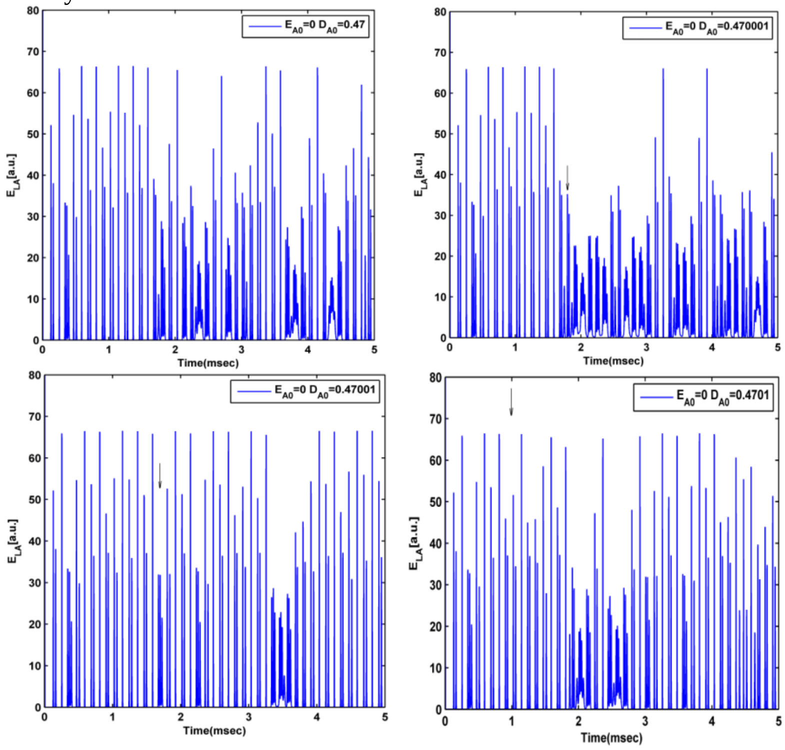

Fig.2 Pure chaos sensitivity to initial conditions.

(a) E_{LA0}=0, D_{A0}=0.47

(b) E_{LA0}=0, D_{A0}=0.470001

(c) E_{LA0}=0, D_{A0}=0.47001

(d) E_{LA0}=0, D_{A0}=0.4701

The ACM model as given in Eq.2(a)-(d) is simulated using same parameters as for CMS except for the addition of message signal in the loop as per Table.1. Quasi-chaos is observed this time with different chaos like time domain plots converging to single trajectory for largely varied values of both E_{LA0} and D_{A0}. D_{A0} is kept at 0.5 and E_{LA0} is changed at four different values i.e. 0, 40, 80 and 120 and result plotted at two time scales in Fig.3 (a) and (b). E_{LA0} is kept at 0 and D_{A0} is changed at four different values i.e. 0.5, 1,-0.5 and -1 and results plotted at two time scales in Fig.3 (c) and (d). It can be observed in all these four figures that the output converges to same trajectory for all these values which is exactly opposite to pure chaos behaviour, which is well known and just seen in CMS simulation. It is to be noted here that chaos outputs are observed here to be more sensitive to D_{A0} changes as compared to E_{LA0} because latter has a smaller scale of variation. However, the output still converges despite using extreme possible values of both E_{LA0} and D_{A0} which proves convergence for all smaller values of initial conditions. Moreover, the results are shown till 2msec only for clarity of diagrams but the convergence is tested to persist till 20 msec once it is achieved. It is believed that convergence will persist forever once achieved. The time of convergence is maximum for E_{LA0} = 80 in Fig. 2(a) and (b) ; not for E_{LA0} = 120 as could be speculated. However, it increases with absolute increase in deviation of D_{A0} from reference D_{A0}=0.5, with D_{A0}=-1 taking longest convergence time of 0.55 msec in Fig. 2(c) and (d).

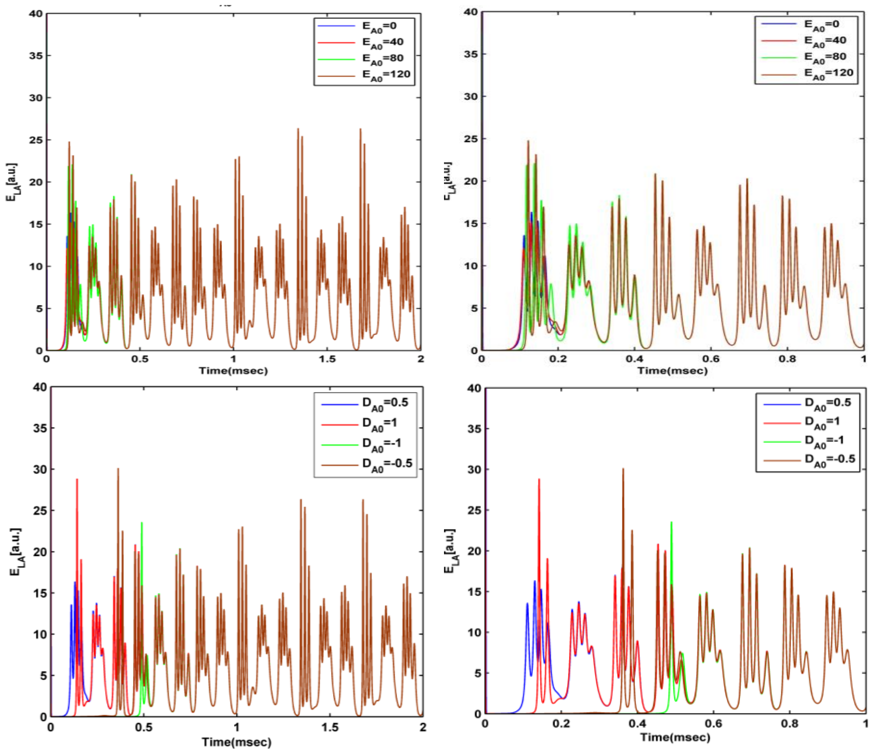

Fig.3 Convergence of quasi-chaos trajectories for different initial conditions.

(a) E_{LA0}=0, E_{LA0}=40, E_{LA0}=80, E_{LA0}=120 and D_{A0}=0.5 (2msec)

(b) E_{LA0}=0, E_{LA0}=40, E_{LA0}=80, E_{LA0}=120 and D_{A0}=0.5 (1msec)

(c) D_{A0}=0.5, D_{A0}=1 D_{A0}=-1 D_{A0}=-0.5 and E_{LA0}=0 (2msec)

(d) D_{A0}=0.5, D_{A0}=1 D_{A0}=-1 D_{A0}=-0.5 and E_{LA0}=0 (1msec)

The time, phase space, frequency, and autocorrelation plots are shown in Fig.4 (a) to (d) for quasi and pure chaos, with system parameters kept same in ACM and CMS, except addition of message in former. The time domain plot of quasi-chaos here is having super pulses with bunches of sub pulses, both being Gaussian, with super pulses being periodic in time but chaotic in amplitude. The time period of sub-pulses is decided by the pump modulating frequency i.e. 9 kHz and there are three to four sub-pulses in every super pulse. Another way of looking at this chaos is considering them as periodic bunches of chaotic Gaussian pulses with humps underneath as reported earlier for loss modulation [5]. The pure chaos has independent Gaussian pulses with no humps underneath and sometimes two or three pulses seem getting merged together due to chaotic timing of pulses themselves. One important indicator of pure pulsed chaos is that it is chaotic in time as well as amplitude while quasi-chaos is chaotic in amplitude only and super and sub pulses are not chaotic in their respective time periods. Each loop in phase space corresponds to a gaussian pulse in time domain. The phase space of quasi-chaos is almost uniformly distributed as the pulses amplitude spreads over a bigger dynamic range. The phase space of pure chaos is spread uniformly on lower amplitudes and then on higher apmplitudes with a gap owing to its temporal signature. Also the DC component and the modulating frequency of 9 kHz are prominent lines in both frequency spectrums, but harmonics of 9 kHz are more prominent in quasi-chaos frequecny spectrum, since the pulse repetition time of quasi-chaos sub-pulses is fixed and is being determined by modulating signal as reported earlier also [6]. The frequency of super pulse and its harmonics is also visible in quasi-chaos spectrum. The pure chaos spectrum is otherwise relatively flatter and richer due to variable chaotic time of pulses. The pure chaos autocorrelation diagrams of both chaos have a sharper decay like earlier while the quasi-chaos autocorrelation function has nonzero lower values in time domain. The fixed time period of chaotic pulses, super and subpulses or bunching and humps and visibility of modulating frequency harmonics in frequency domain are some clues of quasi-chaos revalidated here. There is no fixed linear relationship between delta of initial conditions and time of convergence of trajectories to same trajectory in quasi-chaos.

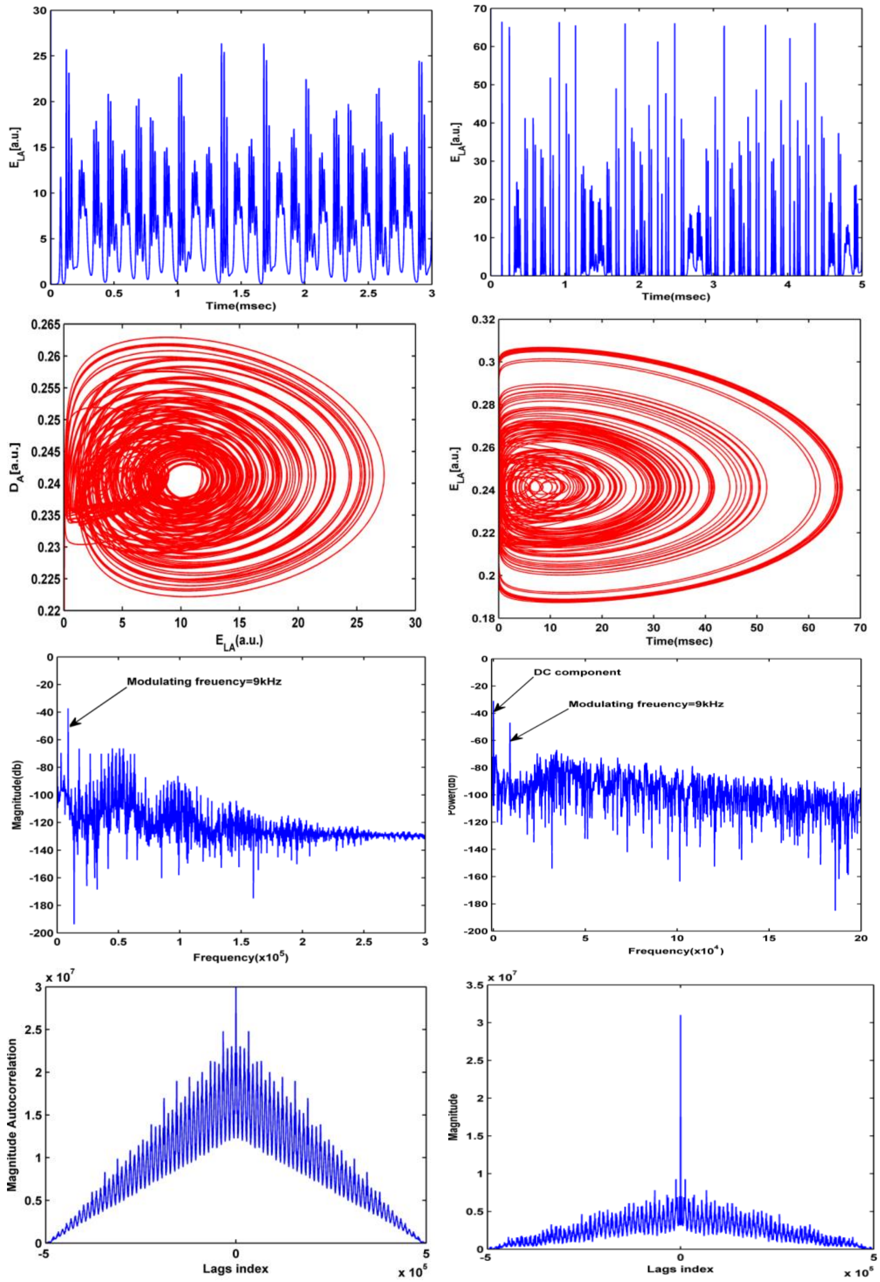

Fig.4 Quasi-chaos (left) vs pure chaos (right) plots
(a) Time domain, (b) Phase space, (c)Frequency domain, (d) Autocorrelation

The time delayed embedded plots of $E_{LA}(t)$ vs $E_{LA}(t\text{-}\tau)$ are shown for different values of time delay τ for quasi-chaos and pure chaos in Fig.5 and 6 respectively with two important observations to be made. Firstly, both of these plots are fractal in nature and the degree of correlation between $E_{LA}(t)$ and $E_{LA}(t\text{-}\tau)$ decreases with the increase in τ in both figures. Secondly, the degree of correlation is lesser in pure chaos as compared to quasi-chaos for corresponding values of τ because randomness and degree of unpredictability is higher in pure chaos. The latter observation is further validated by LE spectrum calculation of both chaos using TISEAN, a well-known routines pack available. We get positive LE for both these types of chaos as shown in Fig.7 (a) and (b) with LE for pure chaos being significantly higher than quasi-chaos which is as expected. This proves that time delayed method of LE calculation will not differentiate between quasi and pure chaos. The only way to identify quasi-chaos is numerically simulating the system with different initial conditions and seeing the time domain plots or physical phase space or physically subjecting the system to different initial conditions if these are accessible in experimental works.

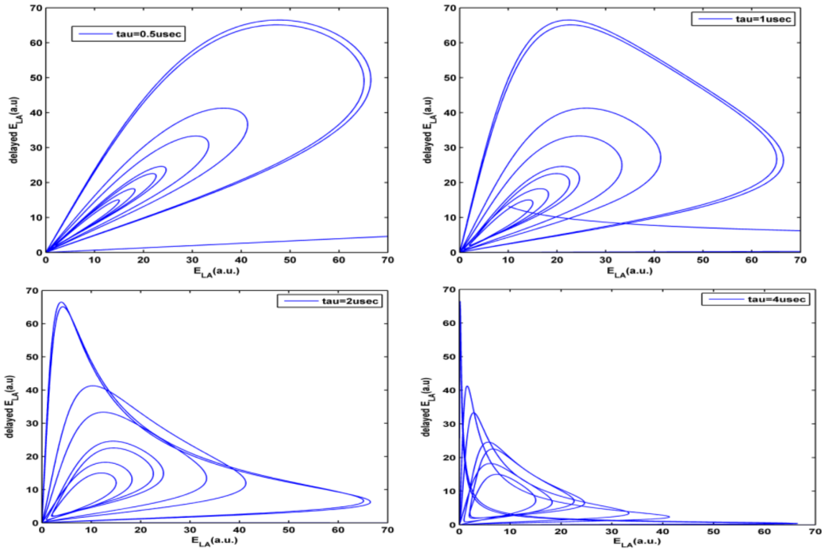

Fig.5 Pure chaos time delayed phase plots
(a) τ = 0.5 usec (b) τ = 1 usec (c) τ = 2 usec
(d) τ = 4 usec

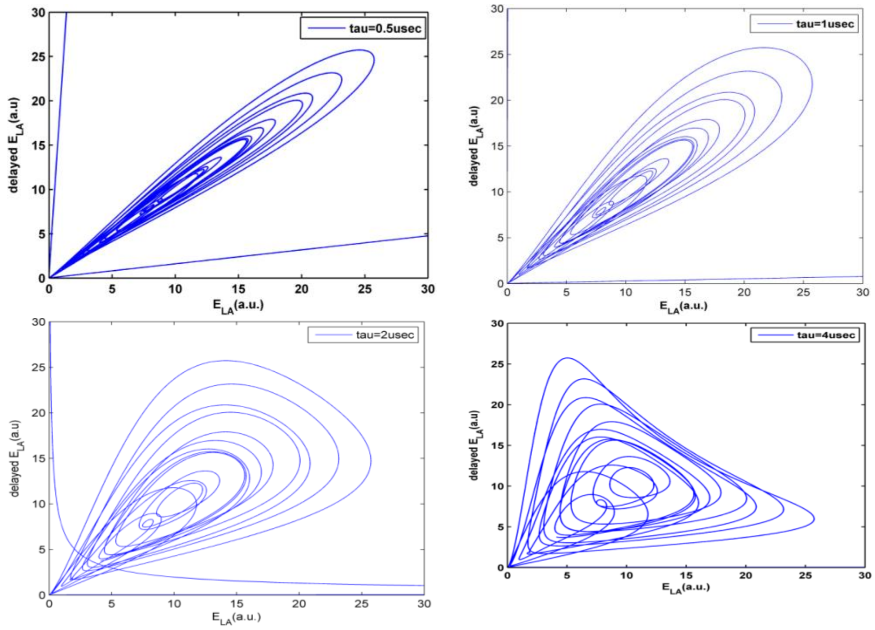

Fig.6 Quasi-chaos time delayed phase plots
(a) τ = 0.5 usec (b) τ = 1 usec (c) τ = 2 usec
(d) τ = 4 usec

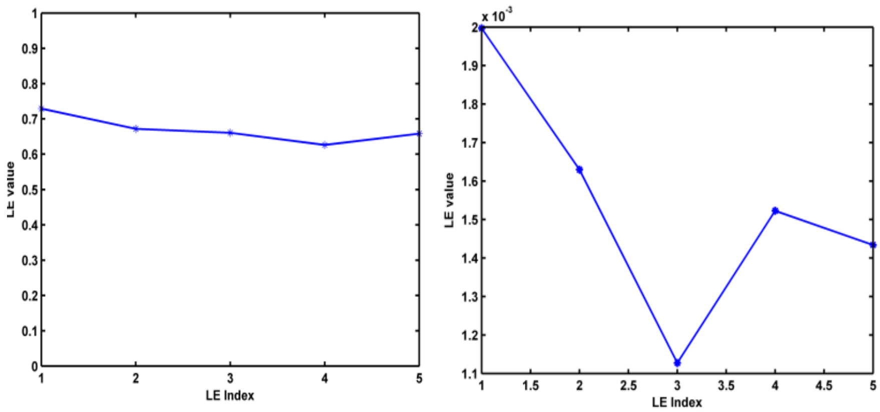

Fig.7 Lyapunov exponent spectrum (a) Pure chaos
(b) Quasi-chaos

IV. Discussion

This numerical investigation is done step-wise on same lines as done earlier [3] for loss modulation scheme and the results are also corresponding, proving the second appearance of quasi-chaos. In order to test the SDIC of pure chaos, the initial condition D_{A0} is varied by very minute differences and the output is still found to diverge even for the slightest of the difference as expected for pure chaos. However, the time of start of divergence of trajectories increases with decrease in difference of D_{A0} which is also anticipated behaviour. On the other hand, quasi-chaos proclaimed to converge instead of diverging, is tested with E_{LA0} and D_{A0} taken to their extreme limits. However, the differently starting trajectories still converge to same single trajectory instead of diverging with the time of convergence increasing this time with the deviation of initial conditions. The message signal adds an extra perturbation in the cavity which is interacting with the loss modulating sine wave, thus producing quasi instead of pure chaos.

The time, frequency, phase space and autocorrelation plots of quasi-chaos once seen independently give an impression of chaos. However, once pure and quasi-chaos plots are observed critically, some differences are observed in respective domains. One major difference is that quasi-chaos has periodic bunches of super pulses while pure chaos pulses, however, are chaotic both in time and in amplitude. Each super pulse has further four sub pulses and the frequency of sub-pulses is fixed at 9 kHz i.e. the modulating frequency. The frequency spectrum of quasi-chaos has all harmonics of both sub and super pulse frequencies while pure chaos spectrum is flatter and richer with better message masking capabilities. The pump modulating frequency is visible in both the spectrums but its harmonics are more vivid in quasi-chaos. The autocorrelation diagram of pure chaos is depicting more randomness due to chaotic timing of pulses. The LE of quasi-chaos calculated using TISEAN are still positive although the physical phase space converges to single trajectory. The reason of this anomaly is the fact that TISEAN calculates LE by creating a pseudo phase space by time delayed embedding of time series data of one physical variable i.e. $E_{LA(t)}$ and $E_{LA(t-\tau)}$ in this case. This pseudo phase space gives positive LE if it is fractal in nature; and it has been found to be fractal in this work not only for pure chaos but also for quasi-chaos. However, the LE values of pure chaos are order of magnitude higher than quasi-chaos. $E_{LA(t)}$ vs $E_{LA(t-\tau)}$ plotted for different values of τ i.e. 0.5 to 4 usec, give fractal plots whose correlation decreases with the increase of τ. The correlation is however, higher in quasi-chaos than pure chaos as the pulses timing is chaotic in latter only.

V. Conclusions

Rediscovery of quasi-chaos in pump modulation scheme in this research, after its first discovery in loss modulation of EDFRL proves that quasi-chaos is also a ubiquitous phenomenon and is the fifth region of operation in nonlinear systems. This work proves that this phenomenon can be traced in all forced chaotic oscillators once the requisite conditions shown here are tuned i.e. one additional sine wave perturbation with frequency not integral multiple of forcing sine wave is added into the system dynamics. Quasi-chaos in this work spoofs itself as a pure chaos by passing all qualitative and visual tests i.e. it has rich spectral content and fast decreasing autocorrelation function and a strange attractor in pseudo phase space. The only visual indicator observed in this work is that pulses are chaotic in amplitude and not in time for quasi-chaos with bunching of pulses into super pulses. The most surprising result in this work is that quasi-chaos gives positive LEs' spectrum using time delayed pseudo phase space analysis of lasing field intensity using TISEAN, a well-known package of LE calculation. Therefore, qualitative visual tests and LE calculations on time delayed series have proven to be a weak test of pure chaos and we need to find stronger quantitative measures of distinguishing pure chaos from quasi-chaos and be cautious with experimental results in forced chaotic systems. The strangely deceptive behaviour of quasi-chaos observed in this work raises many questions from application point of view e.g can quasi-chaos be used for secure chaotic communication and whether to believe experimental data from forced chaotic systems to be pure chaos. Briefly, pure chaos is sensitively dependent on initial conditions both in physical phase space of all dynamic variables and time delayed pseudo phase space of any one physical variable while quasi-chaos is converging in physical phase space and sensitively dependent on initial conditions only in time delayed pseudo phase space.

VI. References

1. A. Argyris, D. Syvridis, L. Larger, V. A. Lodi, P. Colet, I. Fischer, J. G. Ojalvo, C. R. Mirasso, L. Pesquera and K. A. Shore, "Chaos-based communications at high bit rates using commercial fibre-optic links",* Nature, Vol. 438, No. 17, pp. 343-346, November 2005.

2. M. Virte, K. Panajotov, H. Thienpont and M. Sciamanna, "Deterministic polarization chaos from a laser diode" Nature Photonics 2013.

3. S. Z. Ali, "First observation of Quasi-Chaos in Erbium doped fiber ring laser", Chaos Modelling and Simulation (CMSIM) conference, Paris France, May 2015.

4. H. D. I. Abarbanel, M. B. Kennel, M. Buhl and C. T. Lewis, "Chaotic Dynamics in Erbium-doped fiber ring lasers", Physical Review A, Vol. 60 No. 3, pp. 2360-2374, Sep. 1999.

5. S. Z. Ali, M. K. Islam and M. Zafrullah "Effect of Parametric variation on generation and enhancement of chaos in erbium-doped fiber-ring lasers" Optical Engineering Vol. 49 No.10, October 2010.

6. S. Z. Ali, M. K. Islam and M. Zafrullah, "Effect of message parameters in additive chaos modulation in Erbium Doped Fiber Ring Laser ", Optik 124(18), September 2013, pp. 3746-3750.

7. D. Derozier, S. Bielawski and P. Glorieu, “Dynamical behaviour of a doped fiber laser under pump modulation”, Optics Communication, Vol. 83 No. 1,2, pp.97-102, 1991.

8. A. N. Pisarchik , Y. O. Barmenkov, “Locking of self-oscillation frequency by pump modulation in an erbium-doped fiber laser” Optics Communications 254 (2005) 128–137.

9. A. N. Pisarchik, Y. O. Barmenkov and A. V. Kir’yanov , “Experimental Characterization of the Bifurcation structure in an Erbium-Doped Fiber laser with Pump modulation”, IEEE journal of Quantum Electronics, Vol. 39, No. 12, pp. 1567-1571, December 2003.

10. A. N. Pisarchik, A. V. Kir’yanov and Y. O. Barmenkov “Dynamics of an Erbium-doped fiber laser with pump modulation : theory and experiment” Journal of Optical Society of America, Vol. 22, No. 10, pp. 2107- 2114, October 2005.

11. I. J. Sola, J. C. Martin, J. M. Alvarez, “Analytical treatment for the study of an erbium-doped fiber ring laser fed by a sinusoidally modulated pump power”, Optics Communications 258 (2006) 59–66.

12. I. J. Sola, J. C. Martin and J. M. Alvarez, “Nonlinear response of a unidirectional Erbium-doped fiber ring laser to a sinusoidally modulated pump power”, Optics Communication, Vol. 12 , No. 4-6, pp. 359-369, November 2002.

13. A. N. Pisarchik, A. V. Kir’yanov and Y. O. Barmenkov “Dynamics of an Erbium-doped fiber laser with pump modulation : theory and experiment” Journal of Optical Society of America, Vol. 22, No. 10, pp. 2107- 2114, October 2005.

14. L. G. Luo, T. J. Tee and P. L. Chu, “Bistability of Erbium-Doped Fiber Laser”, Optics Communication, Vol. 146 No.1-6, pp. 151-157, 1998.

15. R. Hegger, H. Kantz, and T. Schreiber, “Practical implementation of nonlinear time series methods: The TISEAN package”, Chaos Vol. 9, pp.413-435,1999.